Predictive Threat Assessment via Reachability Analysis and Set Invariance Theory

Paolo Falcone, Mohammad Ali, and Jonas Sjöberg, *Member, IEEE*

***Abstract*—We propose two model-based threat assessment methods for semi-autonomous vehicles, i.e., human-driven vehicles with autonomous driving capabilities. Based on information about the surrounding environment, we introduce a set of constraints on the vehicle states, which are satisfied under "safe" driving conditions. Then, we formulate the threat assessment problem as a constraint satisfaction problem. Vehicle and driver mathematical models are used to predict future constraint violation, indicating the possibility of accident or loss of vehicle control, hence, the need to assist the driver. The two proposed methods differ in the models used to predict vehicle motion within the surrounding environment. We demonstrate the proposed methods in a roadway departure application and validate them through experimental data.**

***Index Terms*—Active safety, decision making, invariant set theory, reachability analysis, semi-autonomous vehicles, threat assessment.**

I. Introduction

CLASSICAL active safety systems, such as yaw stability control, only affect the dynamical behavior of the vehicle, whereas its motion control within the environment is left to the driver. Due to recent advances in sensing technologies [1], [2], modern Advanced Driver-Assistance Systems (ADASs) can instead influence both the dynamical behavior of the vehicle and its motion within the surrounding environment to prevent accidents. In particular, sensor measurements can be fused to obtain information about the surrounding environment, e.g., road geometry and relative position and velocity of moving objects. This is demonstrated in, e.g., [3], where standard radar, which is typically used for adaptive cruise control, is used, along with an *off-the-shelf* camera for joint road geometry estimation and vehicle tracking.

Motivated by the described state of the art in sensing technologies, the current trend in the development of ADASs for passenger cars points toward systems with increased autonomous driving capabilities in complex environments [4], beyond what is currently available in production active safety systems. In particular, future ADASs are envisioned to assist the driver in negotiating curves or intersections and autonomously drive the vehicle to avoid accidents, *if needed*. Prototypes of autonomous vehicles have been shown to successfully accomplish different and complex driving tasks at both low speeds, in urban environments, [5]–[7], and in high-speed maneuvers on low-friction surfaces [8], [9]. The promising results obtained with these prototypes of autonomous vehicles clearly demonstrate the possibilities offered by autonomous driving technologies for active safety applications. However, in active safety applications for passenger cars, it is essential that an assisting autonomous driving intervention is initiated if and only if it is needed, i.e., if a risk of accident is detected that the driver is not able to avoid. The formulation of *transition conditions* between, e.g., manual and fully autonomous driving mode, is not trivial.

In this paper, we consider a threat assessment problem for *semi-autonomous* vehicles, i.e., *human-driven vehicles with autonomous driving capabilities*. We assume that information about the surrounding environment is given with a certain amount of preview and focus on the problem of determining, based on the current vehicle state, whether the driver needs assistance to safely (i.e., without colliding with other objects in the surrounding environment or losing stability) accomplish a driving task.

Although the method is general and can be used in a wide range of accident scenarios, for the sake of easy illustration, in this paper, we consider a lane departure application. In particular, we consider lane guidance systems assisting the driver in maintaining the vehicle within the lane boundaries.

In several lane guidance algorithms, the transition conditions to an autonomous driving mode are formulated based on the *time-to-line crossing* (TLC). An intervention or warning is issued once the TLC passes a predefined threshold. An overview and assessment of methods for calculating the TLC is provided in [10]. Artificial potential fields, instead, are used in the method presented in [11], where lane crossings are prevented by introducing cost functions whose values increase as the vehicle approaches the lane boundaries. An optimization-based approach is presented in [12]. Every time step, based on the current vehicle state and information about the surrounding environment, a Model Predictive Controller (MPC) is used to compute a vehicle trajectory over a future time horizon. An assisting intervention is issued if the computed trajectory is considered hazardous. We observe that, in these approaches, the transition criteria activating the autonomous driving interventions are based on the evaluation of a controller

Manuscript received October 4, 2010; revised April 3, 2011; accepted May 20, 2011. Date of publication July 29, 2011; date of current version December 5, 2011. This work was supported in part by the Vehicle and Traffic Safety Centre (SAFER) at Chalmers University of Technology and in part by Verket för INNOVAtionssystem (VINNOVA) under Project "Systems for Roadway Departure Avoidance." The Associate Editor for this paper was R. I. Hammoud.

P. Falcone and J. Sjöberg are with the Department of Signals and Systems, Chalmers University of Technology, 412 96 Göteborg, Sweden (e-mail: falcone@chalmers.se; jonas.sjoberg@chalmers.se).

M. Ali is with the Department of Signals and Systems, Chalmers University of Technology, 412 96 Göteborg, Sweden, and also with the Active Safety and Chassis Department, Volvo Car Corporation, 405 31 Göteborg, Sweden (e-mail: mali21@volvocars.com).

Color versions of one or more of the figures in this paper are available online at http://ieeexplore.ieee.org.

Digital Object Identifier 10.1109/TITS.2011.2158210

behavior and/or the limitations of the vehicle capability of remaining stable and within the lane, without accounting for the limitations of the driver's ability to perform the same task. This might lead to the initiation of an autonomous driving intervention in situations where the driver does not need assistance. On the other hand, if the controller is outperforming the driver, no intervention might be issued at all. In this paper, instead, we propose two threat assessment methods that explicitly account for the human driving behavior. The idea underlying the proposed methods is to use vehicle and driver mathematical prediction models, along with information about the surrounding environment, to assess the risk of accidents over a future finite-time horizon. We demonstrate the proposed method in a lane guidance application and validate it through experimental data. The paper is organized as follows. In Section II, we provide basic definitions and results on reachability analysis and set invariance theory. In Section III, we present the vehicle and driver modeling used. In Section IV, the threat assessment algorithms are presented. In Section V, we discuss the validation results obtained through the proposed algorithms, whereas Section VI closes the paper with final remarks.

II. Background on Set Invariance Theory and Reachability Analysis

In this section, we introduce a few definitions and recall basic results on set invariance theory and reachability analysis for constrained systems. A comprehensive survey of papers on set invariance theory can be found in [13]. This section adopts the notation used in [14].

We will denote the set of all real numbers and positive integers by $\mathbb{R}$ and $\mathbb{N}^+$, respectively.

Denote by f_a the state update function of an autonomous discrete-time system

$$x(t+1) = f_a\left(x(t), w(t)\right), \tag{1}$$

where $x(t)$ and $w(t)$ denote the state and disturbance vectors, respectively. System (1) is subject to the constraints

$$x(t) \in \mathcal{X} \subseteq \mathbb{R}^n, \quad w(t) \in \mathcal{W} \subseteq \mathbb{R}^d, \tag{2}$$

where $\mathcal{X}$ and $\mathcal{W}$ are polyhedra that contain the origin in their interiors. For the autonomous system (1) and (2),

Definition 1 [Reachable Set (for autonomous systems)]: we define the one-step robust reachable set for initial states x contained in the set $\mathcal{S}$ as

$$\text{Reach}_{f_a}(\mathcal{S}, \mathcal{W}) \triangleq \{x \in \mathbb{R}^n | \exists x(0) \in \mathcal{S}, \exists w \in \mathcal{W} : x = f_a\left(x(0), w\right)\}. \tag{3}$$

For the nominal system, i.e., with $w(t) = 0\ \forall t$, the one-step reachable set is defined as

$$\text{Reach}_{f_a}(\mathcal{S}) \triangleq \{x \in \mathbb{R}^n | \exists x(0) \in \mathcal{S} : x = f_a\left(x(0)\right)\}. \tag{4}$$

For the autonomous system (1) and (2), we define the dual of the reachable set as,

*Definition 2 [*Pre *set (for autonomous systems)]:* the set of states that evolves to $\mathcal{S}$ in one step, i.e.,

$$\text{Pre}_{f_a}(\mathcal{S}, \mathcal{W}) \triangleq \{x \in \mathbb{R}^n | f_a(x, w) \in \mathcal{S} \forall w \in \mathcal{W}\}. \tag{5}$$

For the nominal system, the "Pre" set is defined as

$$\text{Pre}_{f_a}(\mathcal{S}) \triangleq \{x \in \mathbb{R}^n | f_a(x) \in \mathcal{S}\}. \tag{6}$$

Equivalently, for the system with inputs

$$x(t+1) = f\left(x(t), u(t), w(t)\right), \tag{7}$$

subject to constraints

$$x(t) \in \mathcal{X}, \quad u(t) \in \mathcal{U} \subseteq \mathbb{R}^m, \quad w(t) \in \mathcal{W}. \tag{8}$$

Definition 3 [Reachable Set (for systems with external inputs)]: The one-step robust reachable set for initial states x contained in set $\mathcal{S}$ is defined as

$$\text{Reach}_f(\mathcal{S}, \mathcal{W}) \triangleq \{x \in \mathbb{R}^n | \exists x(0) \in \mathcal{S}, \exists u \in \mathcal{U}, \exists w \in \mathcal{W} : x = f\left(x(0), u, w\right)\}. \tag{9}$$

*Definition 4 [*Pre *set (for systems with external inputs)]:* Moreover, we define the set of states that can be driven into the target set $\mathcal{S}$ in one time step as

$$\text{Pre}_f(\mathcal{S}, \mathcal{W}) \triangleq \{x \in \mathbb{R}^n | \exists u \in \mathcal{U} \text{ s.t. } f(x, u, w) \in \mathcal{S}\ \forall w \in \mathcal{W}\}. \tag{10}$$

The sets $\text{Reach}_f(\mathcal{S})$ and $\text{Pre}_f(\mathcal{S})$, for the nominal system with external inputs, are defined similarly as in (4) and (6), respectively.

In this paper, we will use *robust invariant sets* and *robust control invariant sets*. The following definitions are derived from [13], [15], and [16]:

Definition 5 (Robust Positive Invariant Set): A set $\mathcal{O}$ is said to be a positive invariant set for the autonomous system (1) subject to the constraints in (2) if

$$x(0) \in \mathcal{O} \Rightarrow x(t) \in \mathcal{O}, \qquad \forall t \in \mathbb{N}^+. \tag{11}$$

Definition 6 (Maximal Positive Invariant Set $\mathcal{O}_\infty$): The set $\mathcal{O}_\infty$ is the maximal invariant set of the autonomous system (1) subject to the constraints in (2) if $0 \in \mathcal{O}_\infty$, $\mathcal{O}_\infty$ is positive invariant, and $\mathcal{O}_\infty$ contains all positive invariant sets that contain the origin.

Control invariant sets are defined for systems subject to external inputs. The following definitions are derived from [13], [15], [16], and [17].

Definition 7 (Control Invariant Set): A set $\mathcal{C} \subseteq \mathcal{X}$ is said to be a control invariant set for the system in (7) subject to the constraints in (8) if

$$x(t) \in \mathcal{C} \Rightarrow \exists u(t) \in \mathcal{U} \text{ such that } f(x(t), u(t)) \in \mathcal{C}\ \forall t \in \mathbb{N}^+. \tag{12}$$

Definition 8 (Maximal Control Invariant Set $\mathcal{C}_\infty$): The set $\mathcal{C}_\infty$ is said to be the maximal control invariant set for the system in (7) subject to the constraints in (8) if it is control invariant and contains all control invariant sets contained in $\mathcal{X}$.

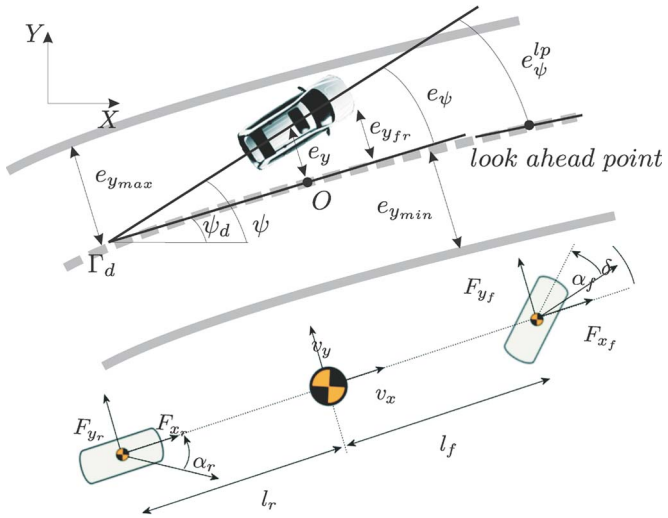

Fig. 1. Vehicle modeling notation.

III. Modeling

In this section, we present the vehicle and driver's steering behavior mathematical models used in Section IV as basis of the threat assessment algorithm.

A. Vehicle Model

Consider the vehicle model shown in Fig. 1. The vehicle motion within the lane, subject to the lateral and yaw dynamics, is described by the following set of differential equations:

$$m\dot{v}_y = -mv_x\dot{\psi} + 2[F_{y_f} + F_{y_r}], \tag{13a}$$
$$J_z\ddot{\psi} = 2[l_f F_{y_f} - l_r F_{y_r}], \tag{13b}$$
$$\dot{e}_{\psi} = \dot{\psi} - \dot{\psi}_d, \tag{13c}$$
$$\dot{e}_y = v_y + v_x e_{\psi}, \tag{13d}$$

where m and J_z denote the vehicle mass and yaw inertia, respectively, l_f and l_r are the distances of the vehicle center of gravity from the front and rear axles, respectively, v_x and v_y are the longitudinal and lateral velocities, respectively, in the vehicle body frame, and $\dot{\psi}$ is the turning rate, where ψ denotes the vehicle orientation w.r.t. the fixed global frame (X, Y) in Fig. 1. F_{y_f} and F_{y_r} are the lateral tire forces at the front and rear axles, respectively. In (13c) and (13d), e_{ψ} and e_y denote the vehicle orientation and position errors, respectively, w.r.t. the road centerline, and ψ_d is the desired vehicle orientation, i.e., the slope of the tangent to curve Γ_d in the point O. The lateral tire forces in (13a) and (13b) are generated at the tire contact patch and are, in general, nonlinear functions of the vehicle states. In this paper, we compute the lateral tire forces as

$$F_{yi} = -C_i\alpha_i, \qquad i \in \{f, r\}, \tag{14}$$

where C_i are the tire cornering stiffness coefficients at the two axles, and α_i are the tire slip angles, which, for small values, can be approximated as

$$\alpha_f = \frac{v_y + l_f\dot{\psi}}{v_x} - \delta, \quad \alpha_r = \frac{v_y - l_r\dot{\psi}}{v_x}, \tag{15}$$

where δ denotes the front steering angle, as shown in Fig. 1.

Remark 1: The simplified linear tire model (14) well approximates more complex nonlinear tire characteristics [18] for small tire slip angles, i.e., $\alpha_i \in [\alpha_{i_{\min}}, \alpha_{i_{\max}}]$. However, this interval also corresponds to a "normal driving" region, where drivers usually operate [19], [20].

For a given vehicle longitudinal speed v_x, the model (13)–(15) can be compactly written as

$$\dot{x}(t) = Ax(t) + Bu(t) + Ew(t), \tag{16}$$

where $x = [v_y, \dot{\psi}, e_{\psi}, e_y]^T$ and $w = \dot{\psi}_d$ are the state and the disturbance vectors, respectively, and $u = \delta$ is the steering input command.

B. Driver Model

In this section, we consider the vehicle model (16) and present a feedback control law resembling the human driver's steering behavior while performing a lane-following task. The driver model, combined with the vehicle model (16), is used next in Section IV as basis of the proposed threat assessment algorithm. The literature on the modeling of driver steering is rich; early studies on driver modeling date back to the 1960s and demonstrate the importance of preview information for human drivers [21]. McRuer *et al.* were among the first to propose a human driver's steering "preview control" algorithm consisting of a "pursuing" part and a closed-loop correcting part [22]. The various preview control algorithms can be divided into two main groups, depending on whether the "preview signal" is provided as a reference or a disturbance [23]. In this paper, the driver's steering behavior is described by a preview control law, where the "preview signal" enters as a disturbance.

Define the orientation error e_{ψ}^{lp}, w.r.t. the lookahead point in Fig. 1 as

$$e_{\psi}^{\mathrm{lp}} = \psi - \psi_d^{\mathrm{lp}} = e_{\psi} + \Delta\psi_d, \tag{17}$$

where ψ_d^{lp} is the desired orientation at time $t + t_{lp}$, with t being the current time, $\Delta\psi_d = \psi_d - \psi_d^{\mathrm{lp}}$, and t_{lp} the preview time that can be mapped into the preview distance d_{lp} under the assumption of constant speed v_x. We consider the vehicle model (13) and compute the steering angle δ as

$$\delta = K_y e_y + K_{\psi} e_{\psi}^{\mathrm{lp}}, \tag{18}$$

with K_y and K_{ψ} gains that are, in general, time varying and might be updated online. Clearly, $\Delta\psi_d$ in (17) depends on the preview time t_{lp}, which, in our modeling framework, is considered as a parameter of the driver's model and can be identified from experimental data. Recursive least-square estimation results of the driver's model parameters are demonstrated in Section V.

C. Driver Controlled Vehicle Model

We consider the autonomous system obtained by combining the vehicle and driver models (16) and (18), respectively, to be compactly written as

$$\dot{x}_a(t) = A_a x_a(t) + E_a w_a(t), \tag{19}$$

where $x_a = [v_y, \dot{\psi}, e_\psi, e_y]^T$ and $w_a = [\dot{\psi}_d, \Delta\psi_d]^T$ are the state and disturbance vectors, respectively. The definitions of matrices A_a, E_a are straightforward.

D. System Constraints

Next, we define a set of operating conditions, in the space of the states and inputs of systems (16) and (19), corresponding to *stable driving within the lane boundaries*. We denote by $e_{y_{ij}}$, $i \in \{f, r\}$, $j \in \{l, r\}$, the distances of the four vehicle corners from the lane centerline. By assuming small orientation errors, $e_{y_{ij}}$ can be written as

$$e_{y_{fl}} = e_y + \frac{c}{2} + ae_\psi, \quad e_{y_{fr}} = e_y - \frac{c}{2} + ae_\psi, \quad \text{(20a)}$$

$$e_{y_{rl}} = e_y + \frac{c}{2} - be_\psi, \quad e_{y_{rr}} = e_y - \frac{c}{2} - be_\psi, \quad \text{(20b)}$$

where c is the vehicle width, and a and b are the distances of the center of gravity from the front and rear vehicle bumpers, respectively. Furthermore, to avoid possible vehicle instability due to the effects of the tire nonlinearities (see Remark 1), the vehicle can be forced to operate in a region of the state space by limiting the tire slip angles α_i, $i \in \{f, r\}$.

The constraints on the vehicle position and slip angles can then be compactly written as

$$-e_{y_{\max}} \le e_{y_{ij}} \le e_{y_{\max}}, \quad \text{(21a)}$$

$$\alpha_{i_{\min}} \le \alpha_i \le \alpha_{i_{\max}}, \qquad i \in \{f, r\}, \quad j \in \{l, r\}, \quad \text{(21b)}$$

where $e_{y_{\max}}$ is the maximum distance of the vehicle corners from the lane centerline.

The model (13)–(15), subject to constraints (21), describes the stable vehicle motion within the lane. Under such operating conditions, assuming small orientation errors is deemed reasonable.

The constraints (21) can be compactly rewritten for the system (16) as

$$[H_x \; H_u] \begin{pmatrix} x \\ u \end{pmatrix} \le h, \quad \text{(22)}$$

whereas, for system (19), we have

$$H_a x_a \le h_a, \quad H_a = H_x + H_u K, \quad h_a = h - H_u K_\psi \Delta\psi_d. \quad \text{(23)}$$

IV. Threat Assessment via Reachability Analysis and Set Invariance Theory

In this section, we propose two threat assessment methods based on the vehicle and driver modeling presented in Section III. The idea underlying the proposed methods is to first introduce a set of constraints on the vehicle state and input trajectories describing a "safe" driving. For the specific lane guidance application considered in this paper, the constraints are set by the lane boundaries and the stability limits that the vehicle should not exceed, i.e., the inequalities (21). Hence, constraint satisfaction implies that the vehicle is traveling within the lane boundaries in a stable operating region. The threat assessment problem is then reformulated as a constraint satisfaction problem over a future time horizon, which is solved through the predictive model-based methods described next.

Based on the vehicle and driver models, every time step, we calculate a "safe set". This is the set of vehicle states at current time t, which, according to the considered vehicle and driver models, are guaranteed to evolve to a given final set in finite time while satisfying the constraints (21). The safe set is updated in receding horizon, as new information about the surrounding environment is available, e.g., the coming road curvature in our lane guidance application. Once the safe set is computed, a set membership test on the current vehicle state is performed to check whether the vehicle is in the safe set and decide whether the driver needs to be assisted.

We use the reachability analysis and set invariance theory definitions given in Section II for linear systems to calculate the safe sets. Similar ideas can be found in [24] and [25] in the automotive and aerospace fields, respectively. In [24], the authors proposed a collision detection method in autonomous driving. In particular, a traffic scenario is considered, where the path of an autonomous vehicle has to be planned to avoid collisions with other traffic participants, whose future trajectory is unknown. A safe planned path for the autonomous vehicle is required to not intersect the *stochastic reachable sets* computed for each traffic participant, i.e., the set of future positions possibly occupied by the other traffic participants. In [25], a safety analysis of an aircraft autoland system is developed based on the calculation of reachable sets. In the landing phase, the set of aircraft configurations evolving within a safe envelope to the set of acceptable states at touchdown is calculated as a backward reachable set. In this paper, we propose two predictive and model-based threat assessment methods. In particular, in the first approach, the vehicle motion within the lane is described by the vehicle model (16) only, whereas in the second, we assume that the steering angle δ in (16) is generated by the state feedback control law (18) and consider the driver-controlled vehicle model (19). Next, in this section, we will highlight how the difference in the used models reflects on the computational scheme used to compute the safe sets (see Remark 4) and the results of the threat assessment (see Remark 3).

In both approaches, the road curvature is assumed to be known over a future time horizon and to lie within a given set. In particular, we introduce the following assumptions on the disturbance signals w and w_a in (16) and (19), respectively.

Assumption 1: $w(t) \in \mathcal{W}$, $w_a(t) \in \mathcal{W}_a \; \forall t \ge 0$, where $\mathcal{W} \subseteq \mathbb{R}$ and $\mathcal{W}_a \subseteq \mathbb{R}^2$ are polyhedrons that contain the origin in their interiors.

We discretize the model (16) with a sampling time T_s to obtain the following discrete-time constrained system with disturbances:

$$x(t+1) = A^d x(t) + B^d u(t) + E^d w(t) \quad \text{(24a)}$$

$$\text{subject to} \quad [H_x \; H_u] \begin{pmatrix} x(t) \\ u(t) \end{pmatrix} \le h, \quad \text{(24b)}$$

where, for the sake of simple notation, we have denoted the state, the disturbance, and the time index with the same symbols as in the continuous time model (16).

Assumption 2: Every time instant t, the disturbances $w(t)$ and $w_a(t)$ are known over a finite-time horizon of N steps.

We recall that, every time instant t, the second component of the disturbance vector w_a, i.e., $\Delta\psi_d$, is based on the desired orientation ψ_d^{lp} at time $t + t_{lp}/T_s$. This is the desired vehicle orientation at the lookahead point. Hence, Assumption 2 on the disturbance w_a requires the knowledge of the road geometry over a future time horizon $t_{lp}/T_s + N$. We define the set of admissible vehicle states as

$$\mathcal{X}_{\text{feas}} = \left\{ x \in \mathbb{R}^4 : [H_x \; H_u] \begin{pmatrix} x \\ u \end{pmatrix} \leq h \right\}. \tag{25}$$

Every time instant, we consider a terminal target set $\mathcal{T} \subseteq \mathcal{X}_{\text{feas}}$. Further details about the choice of $\mathcal{T}$ are provided next, in Section IV-A. Moreover, denote by $W_t = [w_t, w_{t+1}, \ldots, w_{t+N-1}]$ the sequence of disturbance samples over the time horizon $[t, t+N-1]$ and by $W_{t,i} = [w_{t+i}, \ldots, w_{t+N-1}]$ any sequence extracted from W_t. We compute the sequence of states sets $X_t(W_t) = [\mathcal{X}_t, \mathcal{X}_{t+1}, \ldots, \mathcal{X}_{t+N-1}]$ as

$$\mathcal{X}_{t+i}(W_{t,i}) = \mathcal{X}_{\text{feas}} \bigcap \text{Pre}_f(\mathcal{X}_{t+i+1}, w_{t+i}), \quad i = N-1, \ldots, 0, \tag{26a}$$

$$\mathcal{X}_{t+N} = \mathcal{T}, \tag{26b}$$

where f denotes the right-hand side of (24a). We call the set $\mathcal{X}_t$ the *safe set* at time t.

The calculation of sequence $X_t(W_t)$ is performed every time step based on the updated disturbance sequence W_t. In the set operator $\text{Pre}_{\cdot}(\cdot,\cdot)$ in (26), with a slight abuse of notation, a vector is used as second argument, instead of a set. This corresponds to the case of known disturbance.

In summary, the proposed threat assessment algorithm is made of three main steps performed every time instant.

1) Select the terminal target set $\mathcal{T}$.
2) Based on the future disturbance sequence W_t and the set $\mathcal{T}$, perform backward calculation of the sequence of safe sets $\mathcal{X}_{t+i}$ according to (26).
3) Check whether the current state $x(t)$ belongs to the safe set $\mathcal{X}_t$ to assess the driver's ability to safely drive the vehicle from the current state to the target set $\mathcal{T}$ over the future horizon of N steps.

The steps of the method are detailed in Algorithm 1. By construction, if the state of the system (24) at the current time t belongs to the safe set $\mathcal{X}_t$ (Step 10 of Algorithm 1), a steering controller exists such that the vehicle can be driven over the next N time steps while operating within its stability limits and without leaving the lane. That is, over the future N time steps, the vehicle can be driven within the lane boundaries while operating in a region of the system states and inputs space *where the driver is deemed capable of driving without losing vehicle stability* (see Remark 1).

Algorithm 1 is based on the vehicle model (16). Algorithm 2 proposed next, instead, is based on the driver controlled vehicle model (19). In this case, the calculation of the safe sets is based on the reachable and invariant sets for autonomous systems, which are defined in Section II.

Algorithm 1: **Input**: Current state $x(t)$, target set $\mathcal{T}$, sequence of disturbances W_t, state update mapping $f = (A^d, B^d, E^d)$, and constraint matrices (H_x, H_u, h).
Output: The safe set $\mathcal{X}_t$ at the current time t and safe flag $Safe$.
1 **let** $\mathcal{X}_{t+N} = \mathcal{T}$,
2 **for** $i = N-1$ to 0
3 **let** $\mathcal{X}_{t+i+1} = \{x \in \mathbb{R}^4 : H_{i+1}x \leq h_{i+1}\}$,
4 $\text{Pre}_f(\mathcal{X}_{t+i+1}, w_{t+i}) = \{x \in \mathbb{R}^4 : \exists u \in \mathbb{R}$ subj. to $[H_{i+1}A^d \; H_{i+1}B^d]\binom{x}{u} \leq [h_{i+1} - H_{i+1}E^d w_{t+i}]\}$,
5 **if** $\text{Pre}_f(\mathcal{X}_{t+i+1}, w_{t+i}) = \emptyset$ **then** $Safe = 0$, EXIT
6 **else let** $\text{Pre}_f(\mathcal{X}_{t+i+1}, w_{t+i}) = \{x \in \mathbb{R}^4 : H_{\text{Pre}}x \leq h_{\text{Pre}}\}$
7 $\mathcal{X}_{t+i}(W_{t,i}) = \left\{ x \in \mathbb{R}^4 : \begin{bmatrix} H_{\text{Pre}} & \mathbf{0} \\ H_x & H_u \end{bmatrix} \begin{pmatrix} x \\ u \end{pmatrix} \leq \begin{bmatrix} h_{\text{Pre}} \\ h \end{bmatrix} \right\}$, **end**
8 **if** $\mathcal{X}_{t+i}(W_{t,i}) = \emptyset$ **then** $Safe = 0$, EXIT, **end**
9 **end**
10 **if** $x(t) \in \mathcal{X}_t$ **then** $Safe = 1$,
11 **else** $Safe = 0$, **end**
12 EXIT.

We discretize the model (19) with a sampling time T_s to obtain the following discrete-time constrained autonomous system with disturbances:

$$x_a(t+1) = A_a^d x_a(t) + E_a^d w_a(t) \tag{27a}$$

$$\text{subject to} \quad H_a x_a(t) \leq h_a, \tag{27b}$$

where, for the sake of simple notation, we have again denoted the state, the disturbance, and the time index with the same symbols as in (19). With a slight abuse of notation, we let $\mathcal{X}_{\text{feas}}$, $\mathcal{X}_t$, and $\mathcal{T}$ denote the set of admissible states, the safe set at time t, and the terminal set, respectively, for system (27). For system (27), the set of admissible states is defined as

$$\mathcal{X}_{\text{feas}} = \{x \in \mathbb{R}^4 : H_a x \leq h_a\}. \tag{28}$$

The sequence of safe sets for the constrained system (27) is then computed through (26), where the mapping f is replaced by the mapping f_a, denoting the right-hand side of (27a), and the disturbance vectors w_i are replaced by w_{a_i}.

The steps of the threat assessment based on the vehicle and driver's models presented in Section III-A and B, respectively, are detailed in Algorithm 2.

Remark 2: If the safe set $\mathcal{X}_t$ is empty (Steps 5 and 7 of Algorithm 2) or if the current state $x_a(t)$ does not belong to the safe set $\mathcal{X}_t$ (Steps 9 and 10 of Algorithm 2), there exists no state trajectory of system (16) that, under the driver's steering feedback control law (18), can evolve from the current state $x_a(t)$ to the target set $\mathcal{T}$ while satisfying the constraints (21). On the other hand, a different—in general, time-varying—steering law might exist, driving the vehicle from the current state $x_a(t)$ to

the target set while satisfying the constraints (21). The existence of such steering law can be verified through Algorithm 1.

Algorithm 2: **Input**: Current state $x_a(t)$, target set $\mathcal{T}$, sequence of disturbances W_t, state update mapping $f_a = (A_a^d, E_a^d)$, and constraint matrices (H_a, h_a).
Output: The safe set $\mathcal{X}_t$ at the current time t and safe flag $Safe$.
1 **let** $\mathcal{X}_{t+N} = \mathcal{T}$,
2 **for** $i = N-1$ to 0
3 **let** $\mathcal{X}_{t+i+1} = \{x_a \in \mathbb{R}^4 : H_{i+1}x_a \leq h_{i+1}\}$,
4 $\mathrm{Pre}_{f_a}(\mathcal{X}_{t+i+1}, w_{t+i}) = \{x_a \in \mathbb{R}^4 : H_{i+1}A_a^d x_a \leq h_{i+1} - H_{i+1}E_a^d w_{t+i}\}$
5 **if** $\mathrm{Pre}_{f_a}(\mathcal{X}_{t+i+1}, w_{t+i}) = \emptyset$ **then** $Safe = 0$, EXIT
6 **else** $\mathcal{X}_{t+i}(W_{t,i}) = \left\{ x_a \in \mathbb{R}^4 : \begin{bmatrix} H_{i+1}A_a^d \\ H_a \end{bmatrix} x_a \leq \begin{bmatrix} h_{i+1} - H_{i+1}E_a^d w_{t+i} \\ h_a \end{bmatrix} \right\}$, **end**
7 **if** $\mathcal{X}_{t+i}(W_{t,i}) = \emptyset$ **then** $Safe = 0$, EXIT, **end**
8 **end**
9 **if** $x_a(t) \in \mathcal{X}_t$ **then** $Safe = 1$,
10 **else** $Safe = 0$, **end**
11 EXIT.

Remark 3: In Algorithm 2, the restriction of the steering law to the class of linear state feedback control laws (18) leads to smaller safe sets compared with Algorithm 1.

The oversimplified driver model (18) might not be able to capture the driver's steering behavior in hazardous scenarios such as when (i) he/she is required to drive beyond the vehicle stability limits or when (ii) he/she is distracted or drowsy. Nevertheless, for the threat assessment problem formulation considered in this paper, we believe that it is not necessary to exhaustively describe the driver's behavior. In fact, if the vehicle is either beyond its stability limits or the lane boundaries, i.e., Case (i), a threat assessment problem is not meaningful any longer, and an assisting intervention has to be issued. In Case (ii), since our threat assessment problem formulation is not dependent on any driver-monitoring system, driver's distraction or drowsiness is not accounted for. Hence, an assisting intervention would not be issued as long as the vehicle can be maintained within its stability limits and the lane boundaries by the considered "nominal" driver (i.e., behaving according to model (18)). However, the vehicle, which is driven by the drowsy or distracted driver, would very likely eventually exit the "safe set," calculated based on the "nominal" driver behavior, thus enabling the activation of a lower level intervention.

Remark 4: We observe that Steps 4 and 7 of Algorithm 1 involve a projection operation, whereas Algorithm 2 does not. In general, the projection operation can be quite involving, depending on the dimension of the state and input spaces.

In the proposed approaches, we formulate the threat assessment problem as a constraint satisfaction problem, for which efficient methods [26] exist. In particular, we calculate polyhedral representations of the safe sets rather than just assessing the constraint satisfaction for the current vehicle state and the road curvature over the prediction horizon. A polyhedral representation of the safe set can be exploited for both control and verification purposes.

As last remark of this section, we observe that Algorithm 2 assesses the capability of a driver, whose steering behavior is modeled by (18), of driving the vehicle, which is modeled by (16), from the current state $x_a(t)$ to the target set $\mathcal{T}$. Hence, just like in Algorithm 1, constraint satisfaction is not guaranteed after time $t+N$. In the next section, we comment the choice of the target set $\mathcal{T}$ and propose a method for guaranteeing persistent constraint satisfaction, i.e., that the driver will maintain the vehicle within $\mathcal{T}$ for $t > t+N$.

A. Terminal Set

The choice of terminal set $\mathcal{T}$ in the threat assessment Algorithms 1 and 2 affects the *effectiveness* and the *conservativeness* of the algorithms. Indeed, the simplest choice is setting $\mathcal{T} = \mathcal{X}_{\text{feas}}$. In this case, Algorithms 1 and 2 can be used to assess the driver's ability of safely driving only over the future N time steps. As an alternative, for Algorithm 1, the set $\mathcal{T}$ could be chosen as $\mathcal{T} = \mathcal{C}_\infty$, where $\mathcal{C}_\infty \subseteq \mathcal{X}_{\text{feas}}$ is the maximal robust control invariant set for the constrained system with inputs (24). We recall that, in this case

$$x(t+N) \in \mathcal{C}_\infty \Rightarrow x(t+N+k) \in \mathcal{C}_\infty, \qquad \forall w(t) \in \mathcal{W}, \quad k \in \mathbb{N}^+,$$

i.e., *the vehicle will be kept within the lane and its stability limits, despite all admissible lane curvature beyond the lookahead point*. Similarly, for Algorithm 2, the set $\mathcal{T}$ could be chosen as $\mathcal{T} = \mathcal{O}_\infty$, where $\mathcal{O}_\infty \subseteq \mathcal{X}_{\text{feas}}$ is the maximal robust positive invariant set for the constrained autonomous system (27). In this case

$$x_a(t+N) \in \mathcal{O}_\infty \Rightarrow x_a(t+N+k) \in \mathcal{O}_\infty, \qquad \forall w_a(t) \in \mathcal{W}_a,$$

i.e., *the driver is deemed capable of keeping the vehicle within the lane and its stability limits, despite all admissible lane curvature beyond the lookahead point*. Nevertheless, setting the final set equal to the maximal robust control invariant set or the maximal robust positive invariant set for Algorithms 1 and 2, respectively, might lead to high conservativeness of the threat assessment algorithms.

V. Results

The algorithms presented in Section IV have been experimentally validated, and the results are shown in this section. Data have been logged by driving a Volvo V50 along the test track shown in Fig. 2. This track is narrow in several sections and has many sharp curves, thus resembling a country road. The logged data has then been postprocessed offline through Algorithms 1 and 2 to calculate the safe sets along the track. For the sake of brevity, the computed safe sets will be shown only for the vehicle positions along the track, which are marked in Fig. 2 with numbers 1–6, where the vehicle either approaches or travels along a curve.

Data have been collected to calculate the state and the disturbance variables of the vehicle models (16) and (19). In particular, the vehicle lateral velocity v_y and yaw rate $\dot{\psi}$ have

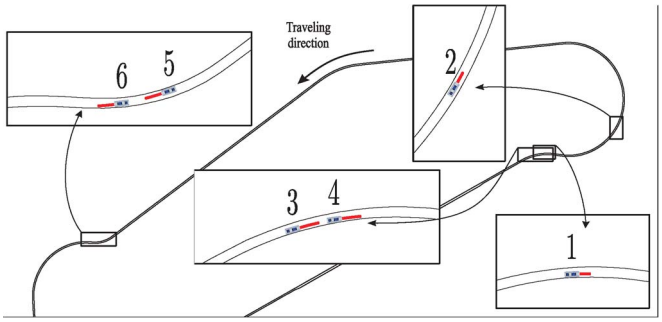

Fig. 2. Test track used for the experimental validation. Validation results of Algorithms 1 and 2 are shown when the vehicle is in the marked positions.

been measured through a high-precision inertial measurement unit. The vehicle position and orientation errors within the lane e_y and e_ψ, respectively, and the desired orientation at the lookahead point ψ_d^{lp} are calculated through dual-antenna Global Positioning System measurements and a digital map including the road geometry.

Remark 5: The set of measurements used in the proposed threat assessment methods could also be obtained online by using the measurement setup and the sensor fusion algorithms used in [1]–[3] (see Section I). Nevertheless, depending on the combination of sensor sets and sensor fusion algorithms, a lower accuracy set of measurements might be obtained compared to the data used in this paper for the validation of the proposed threat assessment algorithms.

We first present the validation results of the driver model (18). The data used for parameter estimation have been collected in both normal and slightly rougher driving styles. Compared with the *normal driving* case, where the driver has been asked to drive according to the suggested road speed limits, in the *rough driving* case, the driver was asked to drive as fast as possible. The problem of estimating parameters K_y, K_ψ, and t_{lp} in (18) has been formulated as a recursive nonlinear least-square problem since the driver model is linear only in parameters K_y, K_ψ. The recursive nonlinear least-square method described in [27] has been used.

Fig. 3(a) shows the identification results under normal driving conditions. We observe high uncertainty in the estimated parameters at the beginning of the considered time interval. The uncertainty is however reduced as soon as the vehicle enters a curve and the system is excited. Moreover, we observe that the estimated value of parameter K_y is very small and has a quite large variance. This indicates that the vehicle lateral deviation from the lane centerline e_y has minor or no influence on the steering angle. The obtained results are in line with the conclusions of previous studies [21], [22] and show that the human-steering behavior is preeminently based on a pursuit component, i.e., based on the preview of the desired path. Fig. 3(b), instead, shows the driver's model parameter estimation in rougher driving maneuvers. Due to higher excitation, the initial uncertainty in the estimated parameters is reduced quicker than in Fig. 3(a). The estimated parameter K_y is, in this case, slightly negative. We also observe a higher magnitude of the estimated parameter K_ψ and a shorter lookahead time t_{lp}, compared to the normal driving case. We conclude that the correcting part is more relevant in rough than in normal driving. The driver model (18) has been used to validate, through experimental data, Algorithm 2.

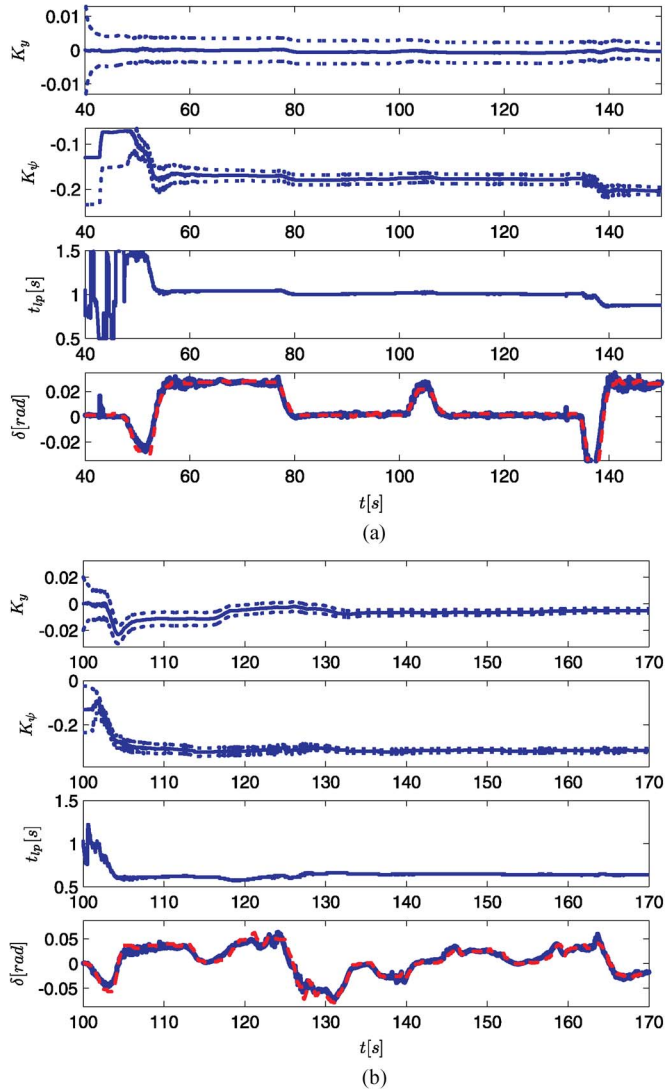

Fig. 3. Recursive driver model parameter estimation. In the two upper plots of (a) and (b), the solid lines show the estimated parameter mean values, whereas the dotted lines show their estimated variances. In the lower plots, the solid and dashed lines show the measured and predicted steering angles, respectively. (a) Normal driving. (b) Rough driving.

TABLE I
VEHICLE AND TIRE DATA USED IN MODEL (16)

m	J_z	l_f	l_r	a
1695 kg	2617 kgm^2	1.14 m	1.50 m	1.83 m
C_f	C_r	b	c	
54 kNm/rad	45 kNm/rad	2.69 m	1.77 m	

Algorithms 1 and 2 have been implemented by setting $\mathcal{T} = \mathcal{X}_{\text{feas}}$ as the terminal set and using the following parameters:

$$\alpha_{f_{\max}} = \alpha_{r_{\max}} = -\alpha_{f_{\min}} = -\alpha_{r_{\min}} = 4^\circ,$$
$$e_{y_{\max}} = 1.56 \text{ m}, \quad N = 35, \quad T_s = 0.01 \text{ s}.$$

The vehicle parameters are shown in Table I.

Remark 6: The calculation of the safe sets shown in this section has been implemented using the set operations

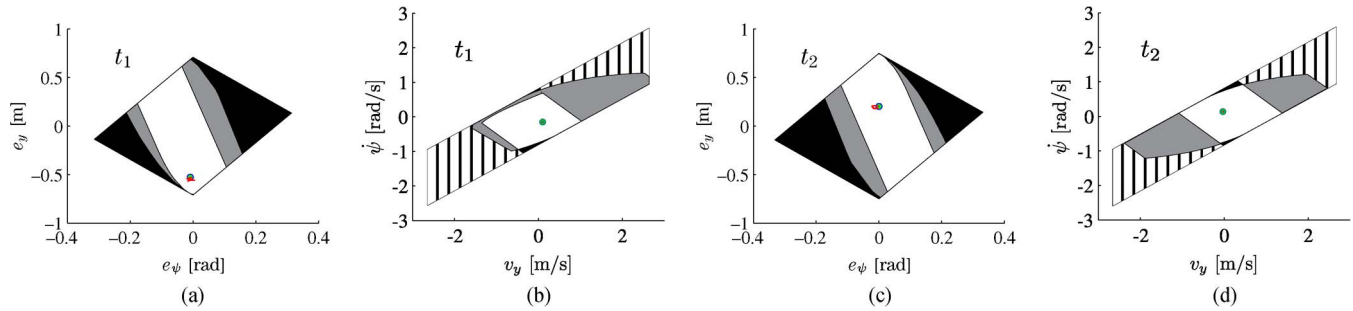

Fig. 4. Safe sets calculated through Algorithms 1 and 2 at times t_1 and t_2. The circles denote the measured current state of the vehicle at time t_1, whereas the solid lines denote the measured state trajectory over the future horizon of N steps. The sets filled with black and white stripes and the sets filled with solid black illustrate cuts of the feasibility sets $\mathcal{T}$ in Algorithms 1 and 2, respectively. The solid gray and white sets show cuts of the safe sets $\mathcal{X}_t$ calculated through Algorithms 1 and 2, respectively.

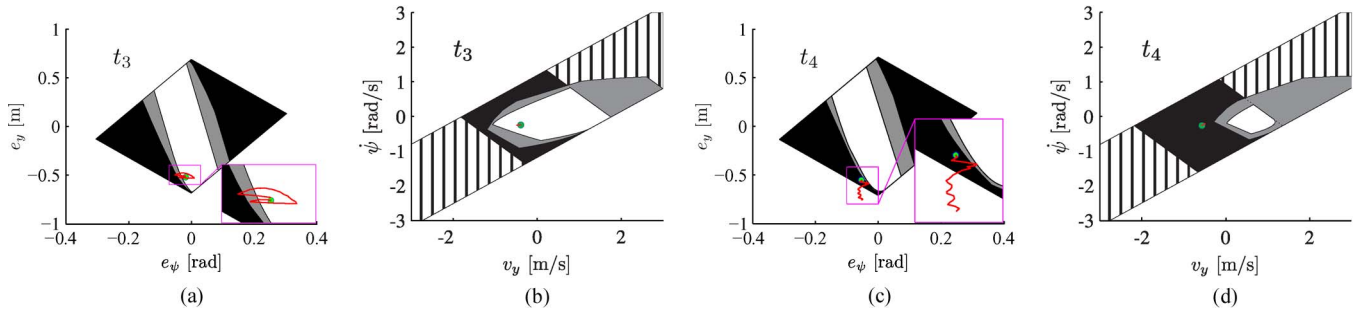

Fig. 5. Safe sets calculated through Algorithms 1 and 2 at times t_3 and t_4. The color convention in Fig. 4 has been used.

implemented in the Multiparametric Programming Toolbox [28]. For the safe set calculation, these operations require 1–2 min for Algorithm 1 and 0.3–0.4 s for Algorithm 2 on a laptop computer.

Consider the driving scenarios 1 and 2 shown in Fig. 2, where the driver is negotiating a curve at a speed of 63 km/h, which can be considered a maneuver requiring normal driving skills.

Denote by t_1 and t_2 the time instants when the vehicle is in positions 1 and 2 on the track, respectively. Fig. 4 shows cuts of the safe sets $\mathcal{X}_{t_1}$ and $\mathcal{X}_{t_2}$ calculated through both algorithms at times t_1 and t_2, respectively.

The following compact notation is introduced to denote set cuts:

$$\mathcal{X}_t^{3,4}(\tau) = \mathcal{X}_t \bigcap \left\{ x \in \mathbb{R}^4 : \begin{bmatrix} 1 & 0 & 0 & 0 \\ 0 & 1 & 0 & 0 \end{bmatrix} x = \begin{bmatrix} x^1(\tau) \\ x^2(\tau) \end{bmatrix} \right\}, \quad (29)$$

where the superscript i in $x^i(\tau)$ denote the ith component of vector $x(\tau)$. The symbol $\mathcal{X}_t^{3,4}(\tau)$ will denote here a set in the $e_y - e_\psi$ space obtained by cutting $\mathcal{X}_t$ at $x^1(\tau)$ and $x^2(\tau)$, i.e., $v_y(\tau)$ and $\dot{\psi}(\tau)$. We observe that, as indicated in Remark 3, the feasibility and safe sets in Algorithm 2 are always enclosed by the corresponding sets in Algorithm 1. This can be explained by recalling that the feasibility and safe sets are derived from the constraints (21), which have been used in both algorithms. Moreover, the inclusion of the driver model (18) in Algorithm 2 results in an additional set of equality constraints, which further limits the set of admissible states.

The states $x(t_1)$ and $x(t_2)$ are marked with a circle in Fig. 4. We observe that, for Algorithm 1, $x(t_1) \in \mathcal{X}_{t_1}^{3,4}(t_1)$, $x(t_1) \in \mathcal{X}_{t_1}^{1,2}(t_1)$, and $x(t_2) \in \mathcal{X}_{t_2}^{3,4}(t_2)$, $x(t_2) \in \mathcal{X}_{t_2}^{1,2}(t_2)$. Hence, from both the initial states $x(t_1)$ and $x(t_2)$, the vehicle is predicted to safely travel over a horizon of N steps. This is confirmed by the vehicle state trajectories measured over the time intervals $[t, t+NT_s]$, $t = \{t_1, t_2\}$ and reported in Fig. 4 with solid lines. In particular, starting from the initial states $x(t_1)$ and $x(t_2)$, the measured vehicle state trajectories entirely evolve over the next N steps within the sets $\mathcal{T}_1$ and $\mathcal{T}_2$, respectively, where $\mathcal{T}_1 = \bigcup_{t=t_1}^{t_1+N-1} \mathcal{T}^{3,4}(t)$, $\mathcal{T}_2$ is similarly defined, and the sets $\mathcal{T}^{3,4}$ are obtained by replacing $\mathcal{X}_t$ with $\mathcal{T}$ in (29), i.e., the vehicle "safely" travels over the time intervals $[t, t+NT_s]$, $t = \{t_1, t_2\}$, as predicted through Algorithm 1. In Fig. 4, we also observe that $x_a(t_1) \in \mathcal{X}_{t_1}$ and $x_a(t_2) \in \mathcal{X}_{t_2}$ when the safe sets are calculated using Algorithm 2. Recall that, for the sake of simple readability, we have adopted the same notation for the safe sets obtained with the two algorithms.

Fig. 5 shows the safe sets $\mathcal{X}_{t_3}$ and $\mathcal{X}_{t_4}$ corresponding to positions 3 and 4 of the track in Fig. 2, when the driver is negotiating a curve at a speed of approximately 92 km/h, traveling close to the lane edge. We observe that, for Algorithm 1, $x(t_3) \in \mathcal{X}_{t_3}$, whereas $x(t_4) \notin \mathcal{X}_{t_4}$. That is, the vehicle is predicted to safely travel over the time interval $[t_3, t_3 + NT_s]$, whereas a constraint violation is predicted over the time interval $[t_4, t_4 + NT_s]$. This is confirmed by the actual vehicle trajectories shown by the solid lines. Similar results are obtained through Algorithm 2 and also shown in Fig. 5. We observe that, starting from position 4, the driver *cuts* the curve to quickly traverse the path. However, such driving behavior might not be considered unsafe, and an intervention should be avoided. Methods for suppressing warnings or interventions have even been proposed in [29] for a lane departure warning system. We observe that, in the framework proposed in this paper, instead,

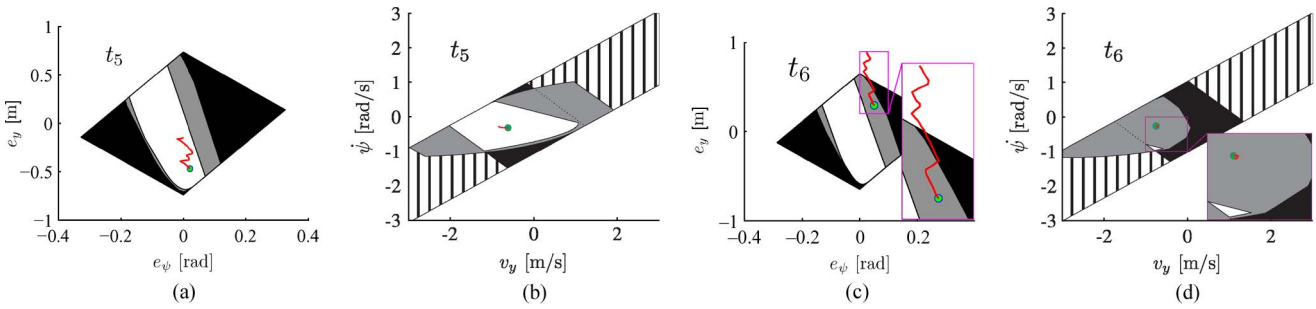

Fig. 6. Safe sets calculated through Algorithms 1 and 2 at times t_5 and t_6. The color convention in Fig. 4 has been used.

warnings or interventions in such driving situations could be avoided by just increasing the bounds $e_{y_{\max}}$, $e_{y_{\min}}$ for the "inner curve" to allow the driver to cut a curve without causing an intervention.

We finally consider vehicle positions 5 and 6 in Fig. 2, where the driver approaches the curve, with a velocity of approximately 84 km/h, which is a very high speed for such a narrow curve. We start with the results obtained with Algorithm 1. In Fig. 6, we observe that $x(t_5) \in \mathcal{X}_{t_5}$ and $x(t_6) \in \mathcal{X}_{t_6}$, which means that there exists a control law that is capable of steering the vehicle over the future N time steps without violating constraints starting from both positions 5 and 6.

The safe set obtained with Algorithm 2, instead, is smaller, compared with that obtained with Algorithm 1, and do not enclose state $x_a(t_6)$. Hence, both algorithms predict safe driving when the vehicle starts from position 5, whereas the results provided by the two algorithms significantly differ in position 6. In this case, Algorithm 2 correctly predicts a constraint violation. In this extreme driving scenario, according to Algorithm 2, the "nominal" driver is not capable of keeping the vehicle in a safe operating region. Depending on his or her driving skills, the actual driver, instead, might succeed in keeping the vehicle in such an operating region by deviating from the "nominal" behavior described by the model (18). Nevertheless, since a deviation from the nominal steering behavior is required, the situation can be considered critical, and an intervention can be motivated.

Remark 7: As anticipated in Remark 2, Algorithm 1 showed that, in position 6, even if the driver is expected to violate constraints, there exists, in general, a time-varying control law that is capable of driving the vehicle over the future N time steps without violating constraints. We conclude that a steering controller could, in this case, be used to assist the driver. The combination of the driver's steering command and of such a low-level steering controller could thus enlarge or move the safe set to enclose state $x(t_6)$.

VI. Conclusion and Future Works

We have presented two model-based threat assessment methods for semi-autonomous vehicles and validated them in a lane guidance application. The two approaches are based on reachability analysis tools and set invariance theory and differ in the model used to predict the vehicle motion within the lane. In particular, in the second algorithm, the driver's steering behavior is estimated based on the road geometry and the vehicle state and used to predict the vehicle motion within the lane. The two methods have been validated offline by using experimental data. The obtained results demonstrate that the proposed methods can effectively predict lane crossing and vehicle instability over a future finite-time horizon, thus allowing the activation of driver assistance systems.

Nevertheless, we point out that

1) Lower accuracy data might be available in an online implementation where a different measurement setup is used (see Remark 5).
2) The proposed algorithms have been tested in a small range of operating conditions.
3) The adopted driver model might not be able to describe the human driver's steering behavior well, thus introducing a high level of uncertainty.
4) The computational burden of the driver's model parameter identification and the safe set calculation might represent an obstacle to the real-time implementation of the proposed algorithms.

Points 1–3 address robustness issues with respect to measurement errors and model uncertainties, whereas point 4 addresses computational complexity issues. The preliminary results presented in this manuscript motivate further investigations, aiming to analyze the impact of measurement errors and model uncertainties on the performance of the proposed threat assessment methods and proposing approaches to compensate for them. Moreover, computational complexity issues will be addressed by adopting real-time oriented code (see Remark 6) and investigating the use of further simplified vehicle models involving simpler reachability analysis problems (see Remark 4).

We finally highlight that, as observed in Remark 7, the proposed threat assessment methods can be a convenient basis of decision-making algorithms, which blend the driver's commands and supporting lower level autonomous driving interventions.

References

[1] J. Jansson, "Collision avoidance theory with application to automotive collision mitigation," Ph.D. dissertation, Dept. Elect. Eng., Linköping Univ., Linköping, Sweden, 2005.
[2] M. Bertozzi, A.Broggi, and A. Fascioli. (2000, Jul.). Vision-based intelligent vehicles: State of the art and perspectives. *Robot. Auton. Syst.* [Online]. vol. 32, no. 1, pp. 1–16. Available: http://linkinghub.elsevier.com/retrieve/pii/S0921889099001256
[3] A. Eidehall, J. Pohl, and F. Gustafsson, "Joint road geometry estimation and vehicle tracking," *Control Eng. Pract.*, vol. 15, no. 12, pp. 1484–1494, Dec. 2007.

[4] U. Mellinghoff, T. Breitling, R. Schöneburg, and H. Metzler, "The Mercedes-benz experimental safety vehicle 2009," in *Proc. Int. Tech. Conf. ESV*, 2009, pp. 1–11.
[5] R. Philippsen, S. Kolski, K. Macek, and R. Siegwart, "Path planning, replanning, and execution for autonomous driving in urban and offroad environments," in *Proc. Workshop Plan., Perception Navigat. Intell. Vehicles (ICRA)*, 2007.
[6] M. Montemerlo, J. Becker, S. Bhat, H. Dahlkamp, D. Dolgov, S. Ettinger, D. Haehnel, T. Hilden, G. Hoffmann, B. Huhnke, D. Johnston, S. Klumpp, D. Langer, A. Levandowski, J. Levinson, J. Marciland, D. Orenstein, J. Paefgen, I. Penny, A. Petrovskaya, M. Pflueger, G. Stanek, D. Stavens, A. Vogt, and S. Thrun, "Junior: The Stanford entry in the urban challenge," *J. Field Robot.*, vol. 25, no. 9, pp. 569–597, Sep. 2008.
[7] C. Baker and J. Dolan, "Traffic interaction in the urban challenge: Putting boss on its best behavior," in *Proc. Int. Conf. IROS*, Sep. 2008, pp. 569–597.
[8] P. Falcone, F. Borrelli, J. Asgari, H. E. Tseng, and D. Hrovat, "Predictive active steering control for autonomous vehicle systems," *IEEE Trans. Control Syst. Technol.*, vol. 15, no. 3, pp. 566–580, May 2007.
[9] P. Falcone, F. Borrelli, H. E. Tseng, J. Asgari, and D. Hrovat, "Integrated braking and steering model predictive control approach in autonomous vehicles," in *Proc. 5th IFAC Symp. Adv. Automot. Control*, 2007.
[10] S. Mammar, S. Glaser, and M. Netto, "Time to line crossing for lane departure avoidance: A theoretical study and an experimental setting," *IEEE Trans. Intell. Transp. Syst.*, vol. 7, no. 2, pp. 226–241, Jun. 2006.
[11] E. J. Rossetter and J. C. Gerdes, "A study of lateral vehicle control under a virtual force framework," in *Proc. Int. Symp. Adv. Vehicle Control*, 2002.
[12] S. J. Anderson, S. C. Peters, T. E. Pilutti, and K. Iagnemma, "An optimal-control-based framework for trajectory planning, threat assessment, and semi-autonomous control of passenger vehicles in hazard avoidance scenarios," *Int. J. Vehicle Auton. Syst.*, vol. 8, no. 2–4, pp. 190–216, 2010.
[13] F. Blanchini, "Set invariance in control—A survey," *Automatica*, vol. 35, no. 11, pp. 1747–1768, Nov. 1999.
[14] P. Grieder, "Efficient computation of feedback controllers for constrained systems," Ph.D. dissertation, Inst. für Automatik, Swiss Fed. Inst. Technol., Zurich, Switzerland, 2004.
[15] D. P. Bertsekas and I. B. Rhodes, "On the minimax reachability of target sets and target tubes," *Automatica*, vol. 7, no. 2, pp. 233–247, Mar. 1971.
[16] D. P. Bertsekas, "Control of uncertain systems with a set–membership description of the uncertainty," Ph.D. dissertation, Electron. Syst. Lab., Mass. Inst. Technol., Cambridge, MA, 1971.
[17] I. Kolmanovsky and E. G. Gilbert, "Theory and computation of disturbance invariant sets for discrete-time linear systems," *Math. Probl. Eng.*, vol. 4, no. 4, pp. 317–367, 1998.
[18] E. Bakker, L. Nyborg, and H. Pacejka, "Tyre modeling for use in vehicle dynamics studies," presented at the Soc. Automotive Eng. (SAE), Detroit, MI, 1987, Paper 870421.
[19] R. Rajamani, *Vehicle Dynamics and Control*. New York: Springer-Verlag, 2006.
[20] U. Kiencke and L. Nielsen, *Automotive Control Systems*. New York: Springer-Verlag, 2005.
[21] R. D. Roland and T. B. Sheridan, "Simulation study of the driver's control of sudden changes in previewed path," Mass Inst. Technol., Dept. Mech. Eng., Cambridge, MA, 1967.
[22] D. T. McRuer, R. W. Allen, D. H. Weir, and R. H. Klein, "New results in driver steering control models," *Hum. Factors*, vol. 19, no. 4, pp. 381–397, Aug. 1977.
[23] H. Peng and M. Tomizuka, "Preview control for vehicle lateral guidance in highway automation," *Trans. ASME, J. Dyn. Syst. Meas. Control*, vol. 115, no. 4, pp. 679–687, Dec. 1993.
[24] M. Althoff, O. Stursberg, and M. Buss, "Model-based probabilistic collision detection in autonomous driving," *IEEE Trans. Intell. Transp. Syst.*, vol. 10, no. 2, pp. 299–310, Jun. 2009.
[25] A. M. Bayen, I. M. Mitchell, and C. J. Tomlin, "Aircraft autolander safety analysis through optimal control-based reach set computation," *J. Guid. Control Dyn.*, vol. 30, no. 1, pp. 68–77, Jan./Feb. 2007.
[26] S. Boyd and L. Vandenberghe, *Convex Optimization*. Cambridge, U.K.: Cambridge Univ. Press, 2004.
[27] S. M. Kay, *Fundamentals of Statistical Signal Processing: Estimation Theory*. Upper Saddle River, NJ: Prentice-Hall, 1993, ser. Prentice Hall Signal Processing Series.
[28] M. Kvasnica, P. Grieder, and M. Baotic, Multi-Parametric Toolbox (MPT), 2004. [Online]. Available: http://control.ee.ethz.ch/~mpt/
[29] X. Dai, A. Kummert, S. B. Park, and D. Neisius, "A warning algorithm for Lane Departure Warning system," in *Proc. IEEE Intell. Vehicles Symp.*, Jun. 2009, pp. 431–435.

Paolo Falcone received the "Laurea" degree in computer science engineering from the Università di Napoli Federico II, Naples, Italy, in 2003 and the Ph.D. degree in automatic control from the Universitá del Sannio, Benevento, Italy, in 2007.

Since April 2008, he has been Assistant Professor in mechatronics with the Department of Signals and Systems, Chalmers University of Technology, Göteborg, Sweden. His research interests include constrained optimal control, real-time model predictive control for fast automotive applications, vehicle dynamics control, and active safety systems.

Mohammad Ali received the M.S. degree in electrical engineering from Chalmers University of Technology, Göteborg, Sweden, where he is currently working toward the Ph.D. degree in mechatronics with the Department of Signals and Systems.

He is also currently with the Active Safety and Chassis Department, Volvo Car Corporation, Göteborg. His current research interests involve active safety and autonomous driving.

Jonas Sjöberg (M'96) received the M.S. degree in engineering physics from Uppsala University, Uppsala, Sweden, in 1989 and the Ph.D. degree from Linköping University, Linköping, Sweden, in 1995.

He has held visiting research positions at the Swiss Federal Institute of Technology Zurich, Zurich, Switzerland; Technische Universitaet Wien, Vienna, Austria; Technion, Haifa, Israel; and Vrije Universiteit, Brussels, Belgium. Since 2001, he has been a Professor with the Department of Signals and Systems, Chalmers University of Technology, Göteborg, Sweden. He is the Program Director of the Automation and Mechatronics Education Program. His research interests are mechatronics and mechatronic-related fields, such as signal processing and control, focusing on model-based methods, simulations, system identification, and optimization for design and product development of mechatronic systems. Current applications are automotive active safety and hybrid electric vehicles.

Dr. Sjöberg has served as an Associate Editor for Control and Control Engineering Practice (1999–2008) and regularly serves as international program committee member at international conferences.